Adsorption (2015) 21:143–151
DOI 10.1007/s10450-015-9657-9

Recovery of *p*-nitrotoluene by selective adsorption using MFI type zeolites

Zhaobing Guo · Shanli Chen · Fengling Liu · Jinjin Wang · Xiaoyu Shen · Shourong Zheng

Received: 23 July 2014 / Revised: 16 December 2014 / Accepted: 13 January 2015 / Published online: 23 January 2015

Abstract Silicalite-1 and HZSM-5 zeolites were used as the adsorbents for selective adsorption of *p*-nitrotoluene (*p*-NT) from simulated wastewater containing *p*-NT and *o*-nitrotoluene (*o*-NT). Results showed that adsorption behaviors of *p*-NT in the zeolites were different from *o*-NT. The maximum adsorption amounts of *p*-NT in the zeolites were found to be approximately 4 molecules per unit cell (mol./u.c.), irrespective of adsorption temperatures investigated, which were markedly higher than those of *o*-NT. In addition, the presence of acid sites led to an enhanced affinity of *p*-NT adsorption and to suppressed adsorption of *o*-NT in HZSM-5 zeolite compared with silicalite-1. Adsorption kinetic results showed that rate constants of *p*-NT were markedly higher than those of *o*-NT in silicalite-1 and HZSM-5 zeolite. For the separation of *p*-NT, enhanced selectivity of HZSM-5 zeolite for *p*-NT adsorption was observed compared with silicalite-1. Under our optimized conditions, *p*-NT with purity of 98.2 % could be recovered with HZSM-5 zeolite, which was ascribed to the marked differences in adsorption amounts and rate constants between *p*-NT and *o*-NT in the zeolite.

Z. Guo (✉) · S. Chen · F. Liu · J. Wang · X. Shen
School of Environmental Science & Engineering; School of Atmospheric Physics, Nanjing University of Information Science & Technology, Nanjing 210044, People's Republic of China
e-mail: guozbnuist@163.com

S. Chen
Environmental Protection Department of Jiangsu Province, Nanjing 210036, People's Republic of China

S. Zheng
State Key Laboratory of Pollution Control and Resource Reuse, School of the Environment, Nanjing University, Nanjing 210093, People's Republic of China

Keywords *p*-nitrotoluene · HZSM-5 zeolite · Silicalite-1 zeolite · Selective adsorption

1 Introduction

Pollution from chemical industry is believed to be one of the main reasons for the deterioration of aquatic environment. In general, most of artificially synthesized chemicals, which usually present in wastewater from chemical processes, are resistant to biodegradation. A variety of studies have demonstrated that the detoxification of wastewater containing these recalcitrant chemicals can be achieved using advanced oxidation processes (AOPs), such as photo-catalysis (Dunlop et al. 2014; Zhang et al. 2013a, b), Fenton oxidation (Liu et al. 2014, Sanchis et al. 2014), ultrasonication (Guo and Feng 2009) and gamma irradiation (Guo et al. 2012). It should be emphasized that the decomposition of these chemicals using AOPs inevitably results in a high treatment cost and waste of resource. Thus, there is a growing need to recover valuable chemicals from wastewater from the viewpoint of cleaner production (Khalili et al. 2014; Xu et al. 2003). Adsorption using solid adsorbents with abundant macro-, meso- and micro-pores is considered as one of appropriate approaches to recover valuable chemicals in wastewater from chemical processes. Generally, a mixture can be recovered if unselective sorbents are employed because wastewater usually contains raw materials, intermediates and products. High purity chemicals can be obtained by further crystallization or distillation if physicochemical properties of these chemicals are markedly different. However, the separation becomes especially difficult if the recovered mixture consists of chemicals with similar properties, such as isomers.

Therefore, direct recovery of high purity chemicals from wastewater using selective sorbents is highly desirable.

MFI type zeolite is a medium-pore aluminosilicate consisting of a three dimensional interconnected channel system with 10-membered openings (0.51 × 0.55 and 0.53 × 0.56 nm). Due to similar dimensions of its channels to dynamic diameter of benzene molecule (0.58 nm), MFI type zeolite is frequently adopted as selective sorbent in aromatic compounds involved processes. Our previous study (Guo et al. 2009) proved that *p*-chloronitrobenzene (*p*-CNB) could be effectively separated from *o*-chloronitrobenzene (*o*-CNB) using silicalite-1 zeolite. It is noteworthy that adsorption selectivity might vary with the properties of the zeolites, such as particle size, Si/Al ratio. In addition, for di-substituted benzene compounds molecular dynamic diameters of *p*-isomers are approximately identical to that of benzene molecule if substituted groups are smaller than benzene molecule. However, molecular diameters of *o*- and *m*-isomers vary with substituted groups, which possibly result in different separation efficiency. Therefore, systematical study on the influence of zeolite properties and dynamic diameters of isomers on separation efficiency is necessary.

p-nitrotoluene (*p*-NT) and *o*-nitrotoluene (*o*-NT), the important intermediates used in the production of plastics, dyes, medicines and pesticides, are produced by toluene nitrification, in which *p*- and *o*-NT with high concentration present in wastewater from washing and dehydration processes. Due to similar kinetic diameter of *p*-NT (0.58 nm) to dimensions of MFI zeolite channels, in the present work, we focused on the recovery of *p*-NT from aqueous solution containing *p*-NT and *o*-NT using HZSM-5 and silicalite-1 zeolite in order to elucidate the influence of zeolite properties on selective adsorption.

2 Experimental

2.1 Materials

Silicalite-1 and HZSM-5 (Si/Al = 50) zeolites were obtained from Kailida Power Industry CO. LTD. China, with average particle diameters of 3 and 5 μm, respectively. *p*-NT and *o*-NT (99.5 %) were purchased from Shanghai Chemicals Factory. All chemicals were used without further purification.

2.2 Adsorption isotherms

Adsorption isotherms of *p*- or *o*-NT in silicalite-1 or HZSM-5 zeolite at different temperatures were determined by batch adsorption experiments. For the determination of *p*-NT adsorption isotherms, zeolite particles with mass varying from 10 mg to 200 mg were charged into the flasks containing 50 mL of *p*-NT aqueous solution (100 mg L^{-1}). For *o*-NT adsorption, 50 mL of *o*-NT aqueous solutions with concentration ranging from 1.25 to 125 mg/L were mixed with 100 mg zeolite sample in the flasks. Then, these flasks were sealed and transferred into an incubator, in which adsorption temperature was controlled at 278, 300 or 320 K. Under continuous shaking, adsorption process was allowed to keep 72 h to reach adsorption equilibrium. Zeolite particles were removed by fast filtration and equilibrium concentrations of *p*- or *o*-NT were determined using a UV–Vis spectrometer (Helios Beta) with detecting wave-length at 288 nm for *p*-NT and at 267 nm for *o*-NT. Adsorption amount of *p*- or *o*-NT in the zeolite was calculated as follows,

$$Q_e = (C_0 - C_e)V/m \quad (1)$$

where Q_e is equilibrium adsorption amount; C_0 is initial concentration; C_e is equilibrium concentration; V is solution volume and m is mass of the zeolite.

2.3 Adsorption kinetics

Adsorption kinetics of *p*- and *o*-NT in the zeolite was evaluated by determining time-resolved uptakes. Typically, 20 mL of distilled water was first mixed with 0.4 g silicalite-1 or HZSM-5 zeolite in a 500 mL flask for 10 min. 380 mL of *p*-NT solution (60 mg/L) was then introduced into the flasks. For the measurements of *o*-NT diffusion, 1.2 g of silicalite-1 or HZSM-5 zeolite was premixed with 20 mL distilled water for 10 min in a 500 mL flask, followed by adding 380 mL of *o*-NT solution (55 mg/L). The mixture was stirred at 300 K. Samples were taken at preset time intervals and zeolite particles were removed by fast filtration. The residual concentration of *p*- or *o*-NT was analyzed spectrophotometrically.

2.4 Selective adsorption

Selective adsorption of *p*-NT from an artificial wastewater containing *p*- and *o*-NT was conducted at 300 K using the zeolites. In a 500 mL flask, 440 mg zeolite sample was suspended in 20 mL distilled water. For selective adsorption of silicalite-1, a mixture of 250 mL 100 mg/L *p*-NT, 100 mL 125 mg/L *o*-NT and 30 mL distilled water was added into the flask. For the adsorption of HZSM-5 zeolite, a mixture of 200 mL 100 mg/L *p*-NT, 160 mL 125 mg/L *o*-NT and 20 mL of distilled water was introduced into the flask. The solution was sampled at different time intervals and residual concentrations of *p*- and *o*-NT in solution were determined using a high-pressure liquid chromatography (Agilent-1100). The detecting wave-length was set at 267 nm and detector temperature at 300 K.

3 Results and discussion

3.1 Adsorption isotherms

The dependencies of adsorption amounts of *p*- and *o*-NT in silicalite-1 and HZSM-5 zeolites on equilibrium concentrations were described in Figs. 1 and 2. Adsorption isotherms of *p*-NT in silicalite-1 and HZSM-5 zeolites showed clear steps at different adsorption temperatures and equilibrium adsorption amounts of *p*-NT where the first step occurred were about 57 mg/g and 55 mg/g (about 2 mol./u.c.), respectively. However, low *o*-NT uptakes were observed in *o*-NT adsorption isotherms, adsorption capacities of *o*-NT in silicalite-1 and HZSM-5 zeolites were around 5 and 2 mg/g at 300 K, indicating different adsorption behaviors of *o*-NT from that of *p*-NT in these two zeolites.

Adsorption isotherms of *p*-NT in the zeolites can be well described using a modified bimodal Langmuir adsorption model:

$$Q_e = Q_1 b_1 C_e/(1 + b_1 C_e) \quad C_e \le C_s \tag{2}$$

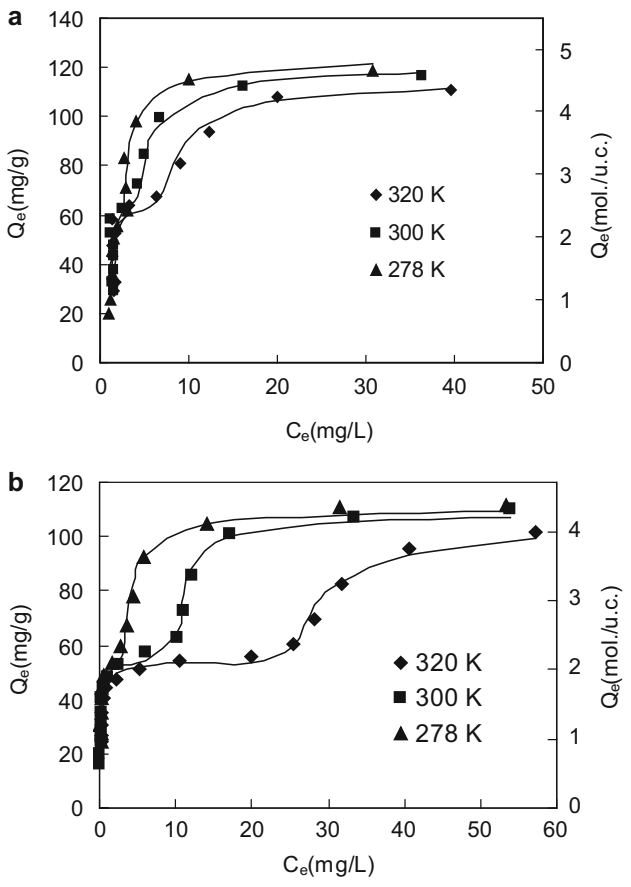

Fig. 1 Adsorption isotherms of *p*-NT in silicalite-1 (**a**) and HZSM-5 zeolites (**b**) at different temperatures (*symbols*: experimental data; *full lines* fitting curves using Eq. 2)

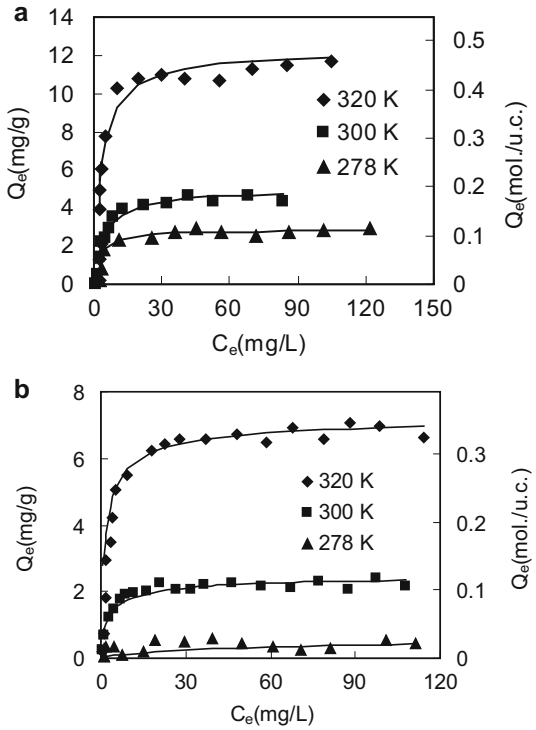

Fig. 2 Adsorption isotherms of *o*-NT in silicalite-1 (**a**) and HZSM-5 zeolites (**b**) at different temperatures (*symbols* experimental data; *full lines* fitting curves using Eq. 3)

$$Q_e = Q_1 b_1 C_e/(1 + b_1 C_e) + Q_2 b_2 (C_e - C_s)/(1 + b_2 (C_e - C_s)) \quad C_e \ge C_s$$

where Q_e is adsorption amount at *p*-NT equilibrium concentration C_e; C_s is the concentration where the first step ends; Q_1 and Q_2 are the maximum adsorption amounts of *p*-NT in different parts of adsorption isotherms; b_1 and b_2 are adsorption parameters, respectively.

In contrast, *o*-NT adsorption in the zeolites fits typical Langmuir- Friendlich adsorption model:

$$Q_e = Q_0 b C_e^n/(1 + b C_e^n) \tag{3}$$

where Q_e is adsorption amount at *o*-NT equilibrium concentration C_e; Q_0 is the maximum adsorption amount; b and n are adsorption parameters, respectively.

The resulting parameters of adsorption isotherms are listed in Tables 1 and 2. From Table 1, the maximum adsorption amounts of *p*-NT in silicalite-1 and HZSM-5 zeolites were found to be about 120 mg/g (4.4 mol./u.c.) irrespective of adsorption temperatures. Thamm (1987) studied gaseous adsorption of aromatic molecules in MFI type zeolite and concluded that benzene, toluene or *p*-xylene was preferentially adsorbed in the intersections of zeolite. Simulation results also revealed that aromatic compounds were usually located in the intersections due to the higher potential energy of *p*-NT adsorbed in the channels compared to that in zeolite intersections (Klemm

Table 1 Parameters of *p*-NT Adsorption Isotherms in silicalite-1 and HZSM-5 Zeolites

Sorbent	T (K)	Q_1		Q_2		$(Q_1 + Q_2)$		b_1 (L/mg)	b_2 (L/mg)	C_s (mg/L)	R^2
		(mg/g)	(mol./u.c.)	(mg/g)	(mol./u.c.)	(mg/g)	(mol./u.c.)				
Silicalite-1	278	56.1	2.2	58.5	2.3	114.6	4.5	2.27	0.95	1.9	0.985
	300	57.7	2.3	53.9	2.1	111.6	4.4	1.85	0.78	4.0	0.953
	320	55.8	2.2	54.3	2.2	110.1	4.4	1.72	0.29	6.5	0.974
HZSM-5 zeolite	278	54.9	2.2	55.2	2.2	110.1	4.4	16.5	0.95	3.3	0.985
	300	55.5	2.2	53.2	2.1	108.7	4.3	7.2	0.8	10.0	0.999
	320	54.3	2.2	53.6	2.1	107.9	4.3	4.6	0.21	24.6	0.978

Table 2 Parameters of *o*-NT Adsorption Isotherms in silicalite-1 and HZSM-5 zeolites

Sorbent	T (K)	Q		b [$(L/mg)^n$]	n	R^2
		(mg/g)	(mol./u.c.)			
Silicalite-1	278	2.87	0.11	0.43	0.98	0.940
	300	5.05	0.20	0.23	0.95	0.955
	320	12.33	0.49	0.33	0.95	0.940
HZSM-5 zeolite	278	0.8	0.03	0.07	0.6	0.902
	300	2.55	0.10	0.50	0.65	0.918
	320	7.27	0.30	0.71	0.72	0.953

et al. 1998). Considering that there are 4 intersections per unit cell of MFI type zeolite, which was identical to the maximum adsorption amounts of *p*-NT in the zeolites, it could be concluded that *p*-NT molecules were located in the intersections of silicalite-1 or HZSM-5 zeolite.

In adsorption isotherms of *p*-NT, clear steps were observed at molecular loadings of 2 mol./u.c. Song and Rees found similar step-like adsorption isotherms of cyclic hydrocarbon in MFI type zeolites and attributed step-like isotherms to intermolecular interactions at high molecular loading (Song and Rees 2000). Therefore, we concluded that step-like isotherms of p-NT in the zeolite is related to intermolecular interactions between *p*-NT molecules due to the longer length of *p*-NT molecule (1.10 nm) than the distance between vicinal intersections of the zeolites (1.0 nm) (Krishna and Paschek 2001). It should be pointed out that b_1 values of *p*-NT adsorption in HZSM-5 are markedly higher compared to those in silicalite-1. However, b_2 values were approximately identical for the zeolites. In principle, b value is characteristic of the affinity of the sorbent for the sorbate. The identical b_2 values were indicative of similar interaction between *p*-NT molecules and zeolite framework. It is noteworthy that Si/Al of HZSM-5 zeolite was 50, indicative of 2 acid sites per unit cell of the zeolite. There is general consensus that acid sites were located in external surface/pore mouth region and the intersections of HZSM-5 zeolite (Epelde et al. 2014). The presence of acid sites in the intersections results in two types of adsorption sites for *p*-NT molecules. It is therefore concluded that at molecular loading higher than 2 mol./u.c. *p*-NT molecules were adsorbed in HZSM-5 intersections without acid sites due to the similar interaction to that of silicalite-1. This suggests that at molecular loading lower than 2 mol./u.c. *p*-NT molecules were preferentially located in HZSM-5 zeolite intersections with acid sites. The high b_1 values in HZSM-5 zeolite are mainly ascribed to extra interaction between *p*-NT molecules and acid sites in the intersections. The preferential adsorption of aromatic molecules in the intersection with acid sites was also observed in gaseous adsorption processes (Thamm 1987; Zhang et al. 2013a, 2013b). Besides, it is found that C_s values of *p*-NT in HZSM-5 zeolite were higher than those in silicalite-1, which was possibly related to strong interaction of *p*-NT molecules with acid sites.

In order to further clarify the interactions between *p*-NT molecules and the zeolites, the dependence of adsorption heats of *p*-NT in HZSM-5 zeolite and silicalite-1 on molecular loadings was obtained using Clausius-Clapeyron equation according to *p*-NT adsorption isotherms (Farrell et al. 2003):

$$\Delta H_{ads} = d\ln(C_e) \Big/ d(1/T)_{Q=const} \tag{4}$$

where ΔH_{ads} is adsorption heat; C_e is equilibrium concentration of *p*-NT at constant adsorption amount Q and T is adsorption temperature, respectively.

The dependence of *p*-NT adsorption heats on molecular loading is described in Fig. 3. Adsorption heats of *p*-NT in

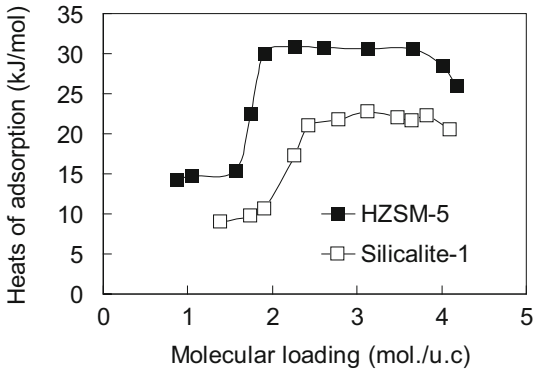

Fig. 3 The dependence of heats of adsorption on *p*-NT molecular loading in silicalite-1 and HZSM-5 zeolites

the zeolites were lower than 40 kJ/mol, indicating that *p*-NT adsorption in the zeolite was a typical physical adsorption process. For *p*-NT adsorption in silicalite-1 and HZSM-5 zeolite, adsorption heats at *p*-NT loadings between 2 and 4 mol./u.c. were found to be higher than those at *p*-NT loadings lower than 2 mol./u.c., which was contributed to the intermolecular interaction (Farrell et al. 2003) at high *p*-NT loadings. At *p*-NT loadings higher than 4 mol./u.c., a decreased adsorption heat was observed, suggesting that *p*-NT molecules were absorbed in the channels or external surface of the zeolites after the intersections were completely occupied.

At *p*-NT loading lower than 2 mol./u.c., adsorption heats of *p*-NT in silicalite-1 and HZSM-5 zeolites were found to be approximately 10 and 15 kJ/mol, respectively. The higher adsorption heats in HZSM-5 zeolite resulted from hydrogen bonding interaction of *p*-NT molecules with SiAlOH groups in zeolite intersections (Farrell et al. 2003).

It can be observed from Tables 1 and 2 that the maximum adsorption amounts of *o*-NT were markedly lower compared to those of *p*-NT. *p*-NT molecules might diffuse into the pores of MFI type zeolite and could be easily adsorbed in the intersections of the zeolite. However, the kinetic diameter of *o*-NT molecule is estimated to be 0.79 nm, which was larger than the dimensions of straight or sinusoidal channels of the zeolite. This might hinder *o*-NT molecules from penetrating into the pores of HZSM-5 zeolite, which led to a decrease in *o*-NT adsorption.

In general, the adsorption of aromatic molecules in MFI type zeolite was considered as a physical adsorption process, which suggested that the adsorption was favorable at low adsorption temperature. This was supported by the results of *p*-NT adsorption in silicalite-1 and HZSM-5 zeolites. However, *o*-NT adsorption was favored at high adsorption temperature, which implied that *o*-NT adsorption in the zeolite was probably controlled by dynamics due to its slightly larger diameter compared to the dimensions of the zeolite channels.

In addition, the higher maximum adsorption amounts of *o*-NT in silicalite-1 were observed compared to those in HZSM-5 zeolite. It is noteworthy that acid sites of MFI type zeolite located in pore mouth region could be detected using different approaches. The acid sites located in the pore mouth region tend to absorb H_2O (Kolvenbach et al. 2011), which led to the narrowing of pore openings of HZSM-5 zeolite and further suppresseed *o*-NT molecules from diffusing into the pores.

3.2 Adsorption kinetics

Adsorption kinetics of sorbate molecules in porous materials can be determined using time-resolved uptake (Zheng et al. 2003). The time-resolved uptakes of *p*- and *o*-NT in the zeolites, measured at 300 K, are depicted in Figs. 4 and 5. It is noted that *p*-NT adsorption in silicalite-1 reached equilibrium at 25 min and *o*-NT within 1,400 min. In HZSM-5 zeolite, adsorption of *p*-NT reached saturation stage at 20 min and *o*-NT within 1,200 min.

The adsorption process can be described by pseudo-first-order or pseudo-second-order kinetics (Smit and Maesen, 2008). For pseudo-first-order kinetics, the Lagergren rate equation is generally used,

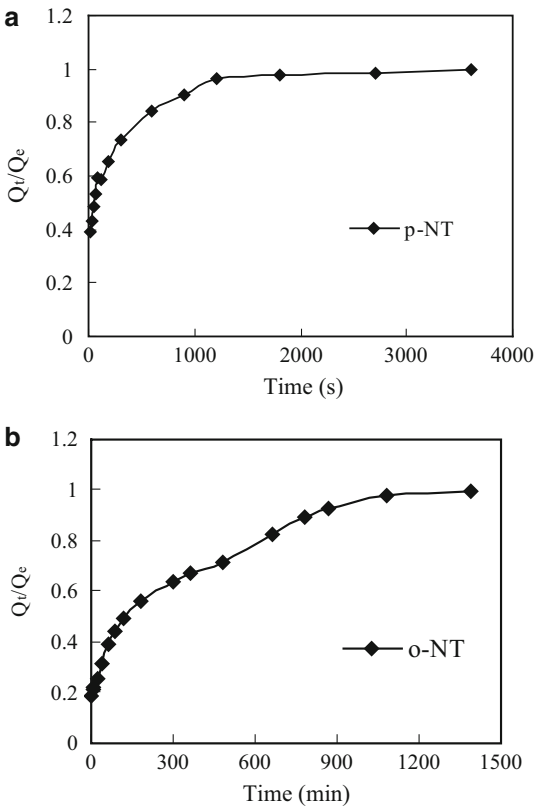

Fig. 4 Adsorption kinetics of *p*-NT (**a**) and *o*-NT (**b**) in silicalite-1

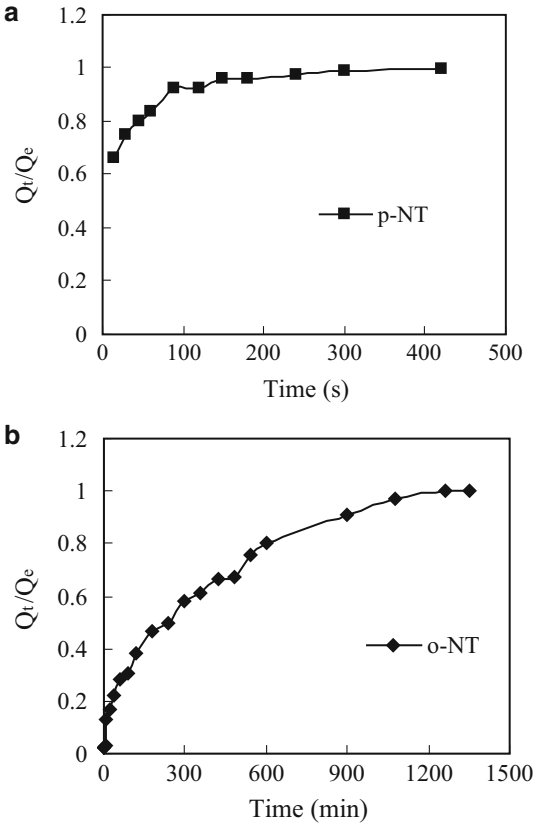

Fig. 5 Adsorption kinetics of *p*-NT (**a**) and *o*-NT (**b**) in HZSM-5 zeolite

$$\log(q_e - q_t) = \log(q_e) - \frac{k_1}{2.303}t \quad (5)$$

The pseudo-second-order kinetics can be expressed as the Eq. (6),

$$\frac{t}{q_t} = \frac{1}{k_2 q_e^2} + \frac{1}{q_e}t \quad (6)$$

where q_e is equilibrium adsorption amount, q_t is adsorption amount at time t, k_1 and k_2 is pseudo-first-order and pseudo-second-order rate constant, respectively.

The plots of log $(q_e - q_t)$ vs t based on pseudo-first-order kinetics and t/q_t vs t based on pseudo-second-order kinetics in the zeolites are compiled in Fig. 6. It is found that the plots of log $(q_e - q_t)$ vs t did not give a linear relation. However, good linear plots of t/q_t vs t suggested that NTs adsorption in the zeolites followed pseudo-second-order kinetic model, and the corresponding simulation parameters are listed in Table 3. In addition, the calculated equilibrium adsorption amounts of NTs in the zeolites according to Eq. (6) in Table 3 were generally identical to experimental results, which further indicated the adsorption of NTs in the zeolites fitted pseudo-second-order kinetic model.

At 300 K, rate constant of *p*-NT in silicalite-1 was 3.69×10^{-2} g/(g min) at equilibrium concentrations of 1.7 mg/L, and rate constant of *o*-NT was 1.41×10^{-3} g/(g min) at equilibrium concentrations of 34.1 mg/L. This indicates that *p*-NT adsorption was approximately 26 times faster compared to that of *o*-NT in the zeolite, which was mainly ascribed to the difference between kinetic diameters of *p*-NT (0.58 nm) and *o*-NT (0.79 nm). Similar results were obtained for *p*- and *o*-NT adsorption in HZSM-5 zeolite. At 300 K, rate constant of *p*-NT in HZSM-5 zeolite was calculated to be 1.31×10^{-1} g/(g min) at equilibrium concentrations of 0.9 mg/L. In contrast, rate constant of *o*-NT was 1.12×10^{-3}g/(g min) at equilibrium concentrations of 49.6 mg/L, indicating that rate constant of *p*-NT was about 120 times higher than that of *o*-NT in HZSM-5 zeolite.

It should be pointed out that rate constant of *p*-NT in silicalite-1 was lower than that in HZSM-5 zeolite. In fact, the measured adsorption rate constant varied in different samples for a given adsorption system (Ruthven 2007; Yu et al. 2013). In particular, a higher rate constant was always observed in zeolite with larger crystals due to the presence of surface barrier in the zeolite with small crystals.

3.3 Selective adsorption

For selective adsorption of *p*-NT from aqueous solution containing *p*- and *o*-NT, time-resolved uptakes of *p*- and *o*-NT in silicalite-1 and HZSM-5 zeolites are compared in Figs. 7 and 8. At 300 K, *p*-NT adsorption in silicalite-1 reached the equilibrium after 30 min with *p*-NT equilibrium concentration at 1.4 mg/L. For *o*-NT, however, it took more than 2,000 min to reach adsorption equilibrium with *o*-NT concentration at 26.8 mg/L, indicating that *p*-NT adsorption was markedly faster compared to that of *o*-NT in the mixture. Compared with equilibrium time in single component adsorption processes under similar equilibrium concentrations, it can be concluded that the presence of *o*-NT in solution had no influence on *p*-NT adsorption in the zeolite. In contrast, the adsorption process of *o*-NT was restrained in the presence of *p*-NT. Furthermore, adsorption amounts of *p*- and *o*-NT in the zeolite were found to be 53.9 and 2.4 mg/g at *p*-NT equilibrium concentration of 1.4 mg/L and *o*-NT of 26.8 mg/L (see Fig. 7). Under the same equilibrium concentrations, adsorption amounts of *p*- and *o*-NT in silicalite-1 were 52.9 and 4.7 mg/g in the single component adsorption processes (see Figs. 1, Fig. 2), indicating that an identical equilibrium adsorption amount for *p*-NT and a decreased adsorption amount for *o*-NT were obtained in the zeolite during the separation process. The enlarged differences in equilibrium adsorption amounts and adsorption time between *p*-NT and *o*-NT in the separation process could be ascribed to high rate

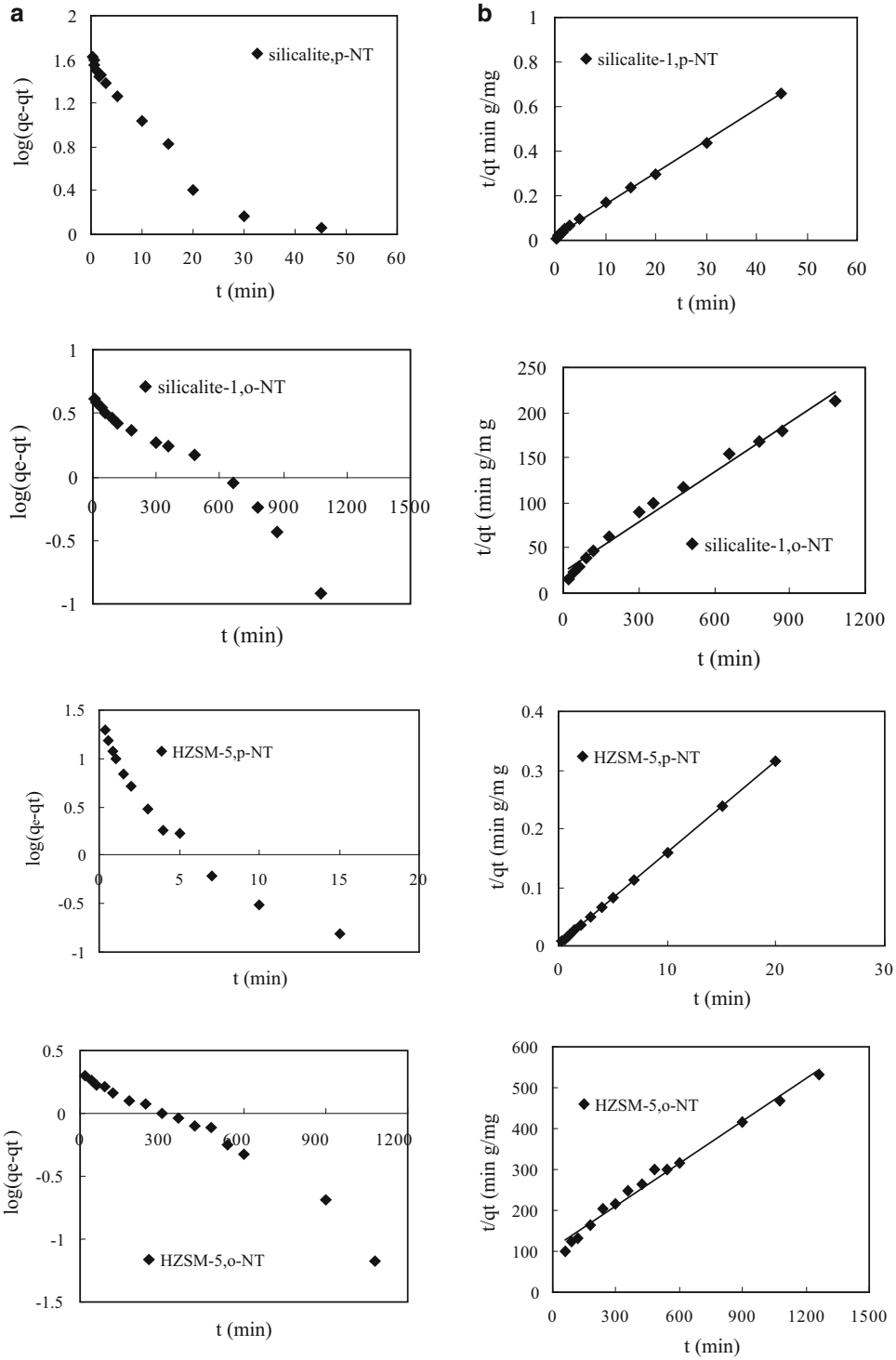

Fig. 6 Simulation of NTs adsorption in the zeolites using **a** pseudo-first-order kinetics and **b** pseudo-second-order kinetics

constant of *p*-NT in silicalite-1. This led to the prior occupation of adsorption sites by *p*-NT in silicalite-1, which inevitably lowered *o*-NT adsorption amount and lengthened its equilibrium adsorption time in silicalite-1.

For selective adsorption in HZSM-5 zeolite at 300 K, adsorption amounts of *p*- and *o*-NT were 44.9 and 1.3 mg/g at *p*-NT equilibrium concentration of 0.6 mg/L and *o*-NT of 49.6 mg/L in the separation process. The equilibrium adsorption time of *p*- and *o*-NT were found to be 20 and 1,500 min, respectively. Compared with the single component adsorption processes, equilibrium adsorption time and adsorption amount of *o*-NT in HZSM-5 zeolite decreased.

Table 3 Pseudo-second-order adsorption rate constants and the calculated and experimental q_e values for adsorption of NTs in the zeolites

Zeolite	NT	C_e (mg/L)	K_2 [g/(g min)]	q_e (exp) (mg/g)	q_e (cal) (mg/g)	R^2
Silicalite-1	*p*-NT	1.7	3.69×10^{-2}	58.3	59.0	0.99
Silicalite-1	*o*-NT	34.1	1.41×10^{-3}	5.1	5.0	0.99
HZSM-5	*p*-NT	0.9	1.31×10^{-1}	49.3	49.0	1
HZSM-5	*o*-NT	49.6	1.12×10^{-3}	2.5	2.9	0.99

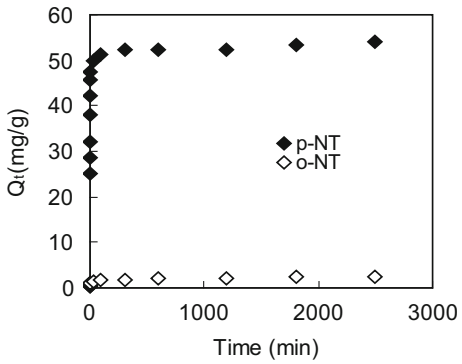

Fig. 7 Time resolved uptakes of *p*- and *o*-NT in silicalite-1 at 300 K

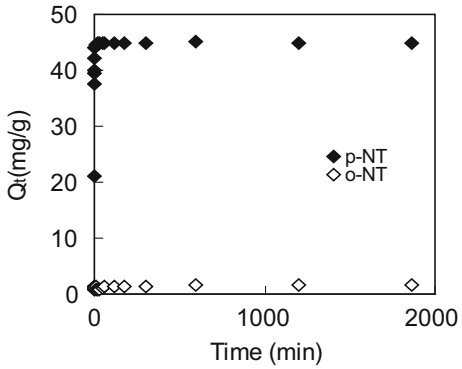

Fig. 8 Time resolved uptakes of *p*- and *o*-NT in HZSM-5 zeolite at 300 K

However, equilibrium adsorption time and adsorption amount of *p*-NT in HZSM-5 zeolite kept identical.

The larger difference in adsorption amounts and equilibrium adsorption time between *p*-NT and *o*-NT could result in higher separation efficiency. The results showed that equilibrium adsorption amounts of *p*- and *o*-NT in silicalite-1 were 53.9 and 2.4 mg/g at 300 K, and residual concentration of *p*- and *o*-NT were 1.4 and 26.8 mg/L, respectively. This revealed that *p*-NT with purity of 95.7 % was selectively adsorbed in silicalite-1 and *o*-NT with purity of 95.0 % in the solution under our separation conditions. Furthermore, the optimum separation for *p*-NT can be achieved at 30 min when *p*-NT reached adsorption equilibrium in silicalite-1. Our results showed that *p*-NT purity could increase up to 96.7 %. Similarly, 97.2 % of *p*-NT and 98.8 % of *o*-NT could be obtained in HZSM-5 zeolite at adsorption equilibrium stage, and 98.2 % of *p*-NT and 99.2 % of *o*-NT could be recovered under optimum adsorption condition. The enhanced recovery efficiency in HZSM-5 zeolite was mainly attributed to the further suppressed adsorption of *o*-NT due to the presence of acid sites in the pore mouth of the zeolite.

For the recovery of *p*-NT, the desorption of *p*-NT from the used zeolite was investigated in this study. Results showed that the desorption efficiency of *p*-NT was higher than 99 % at 300 K with ethanol as the eluate, indicating that *p*-NT desorption was feasible and the used zeolites could be easily regenerated.

4 Conclusions

Selective adsorption of *p*-NT from aqueous solution containing *p*- and *o*-NT using silicalite-1 and HZSM-5 zeolites was investigated. The results revealed that MFI type zeolites were effective adsorbents to separate *p*-NT from *o*-NT in simulated wastewater. For *p*-NT adsorption, molecules preferentially occupied channel intersections of the zeolites. The equilibrium adsorption amounts of *p*-NT were markedly higher than those of *o*-NT in silicalite-1 and HZSM-5 zeolites, and adsorption rate constant of *p*-NT was much faster compared to that of *o*-NT. The significant differences in adsorption amounts and equilibrium adsorption time between *p*-NT and *o*-NT led to high separation efficiency. In addition, the presence of acid sites in the intersections and pore mouth regions of HZSM-5 resulted in an enhanced separation efficiency. Under our experimental conditions, 95.7 % *p*-NT and 95.0 % *o*-NT could be recovered in silicalite-1, and 97.2 % *p*-NT and 98.8 % *o*-NT were obtained in HZSM-5 zeolite.

Acknowledgments We gratefully acknowledge supports from National Natural Science Foundation of China (41373023); Jiangsu Province and research prospective joint research Projects (BY2013007-03); a project funded by the Priority Academic Program Development of Jiangsu Higher Education Institutions; University research project to promote the industrialization of Jiangsu Province and Jiangsu "333 high-level talents project".

References

Dunlop, P.S.M., Ciavola, M., Rizzo, L., McDowell, D.A., Byrne, J.A.: Effect of photocatalysis on the transfer of antibiotic resistance gene in urban wastewater. Catal. Today **49**, 1–6 (2014)

Epelde, E., Gayubo, A.G., Olazar, M., Bilbao, J., Aguago, A.T.: Modified HZSM-5 zeolites for intensifying propylene production in the transformation of 1-butene. Chem. Eng. J. **251**, 80–91 (2014)

Farrell, J., Manspeaker, C., Luo, J.: Understanding competitive adsorption of water and trichloroethylene in a high-silica Y zeolite. Micropor. Mesopor. Mater. **59**, 205–214 (2003)

Guo, Z.B., Feng, R.: Ultrasonic irradiation-induced degradation of low-concentration bisphenol A in aqueous solution. J. Hazard. Mater. **163**, 855–860 (2009)

Guo, Z.B., Zheng, S.R., Zheng, Z.: Separation of p-chloronitrobenzene and o-chloronitrobenzene by selective adsorption using Silicalite-1 zeolite. Chem. Eng. J. **155**, 654–659 (2009)

Guo, Z.B., Dong, Q.Y., He, D.L., Zhang, C.Z.: Gamma radiation for treatment of bisphenol A solution in presence of different additives. Chem. Eng. J. **183**, 10–14 (2012)

Khalili, N.R., Duecker, S., Ashton, W., Chavez, F.: From cleaner production to sustainable development: the role of academia. J. Clean. Prod. **12**, 1–14 (2014)

Klemm, E., Wang, J., Emig, G.: A comparative study of the sorption of benzene and phenol in silicalite, HAlZSM-5 and NaALZSM-5 by computer simulation. Micropor. Mesopor. Mater. **26**, 11–21 (1998)

Kolvenbach, R., Al-Yassir, N., Al-khattaf, S.S., Gobin, O.C., Ahn, J.H., Jentys, A., Lercher, J.A.: A comparative study of diffusion of benzene/p-xylene mixture in MFI particles, pellets and grown membranes. Catal. Today **168**, 147–157 (2011)

Krishna, R., Paschek, D.: Molecular simulations of adsorption and siting of light alkanes in silicalite-1. Phys. Chem. Chem. Phys. **3**, 453–462 (2001)

Liu, H.H., Chen, Q.Y., Zhang, S.H., Li, X.Y.: Relationship of mineralization of amino naphthalene sulfonic acids by Fenton oxidation and frontier molecular orbital energies. Chem. Eng. J. **247**, 275–282 (2014)

Ruthven, D.M.: Transient behaviour of a zeolite membrane under non-linear conditions. Chem. Eng. Sci. **62**, 5745–5752 (2007)

Sanchis, S., Polo, A.M., Tobajas, M., Rodriguez, J.J., Mohedano, A.F.: Coupling Fenton and biological oxidation for the removal of nitrochlorinated herbicides from water. Water Res. **49**, 197–206 (2014)

Smit, B., Maesen, T.L.M.: Molecular simulations of zeolites: adsorption, diffusion, and shape selectivity. Chem. Rev. **108**, 4125–4184 (2008)

Song, L., Rees, L.V.C.: Adsorption and diffusion of cyclic hydrocarbon in MFI-type zeolites studied by gravimetric and frequency-response techniques. Micropor. Mesopor. Mater. **35**, 301–314 (2000)

Thamm, H.: Adsorption site heterogeneity in silicalite: a calorimetric study. J. Phys. Chem. **7**, 341–346 (1987)

Xu, Z., Zhang, Q., Fang, H.H.: Applications of porous resin sorbents in industrial wastewater treatment and resource recovery. Crit. Rev. Environ. Sci. Technol. **33**, 363–389 (2003)

Yu, Y.Z., Gutierrez, O.Y., Haller, G.L., Colby, R., Kabius, B., Alercher, J.: Tailoring silica-alumina-supported Pt-Pd as poison-tolerant catalyst for aromatics hydrogenation. J. Catal. **304**, 135–148 (2013)

Zhang, Y.Y., Xiong, Y., Tang, Y.K., Wang, Y.H.: Degradation of organic pollutants by an integrate photo-Fenton-like catalysis/immersed membrane separation system. J. Hazard. Mater. **244**, 758–764 (2013a)

Zhang, Q., Tan, Y., Yang, C., Xie, H.J., Han, Y.Z.: Characterization and catalytic application of MnCl2 modified HZSM-5 zeolites in synthesis of aromatics from syngas via dimethyl ether. J. Ind. Eng. Chem. **19**, 975–980 (2013b)

Zheng, S.R., Heydenrych, H.R., Jentys, A.J., Lercher, A.: On the enhanced selectivity of HZSM-5 modified by chemical liquid deposition. Top. Catal. **22**, 101–106 (2003)